ELSEVIER

Catalysis Today 53 (1999) 715–723

CATALYSIS TODAY

www.elsevier.com/locate/cattod

Kinetics and mechanism of low-temperature ozone decomposition by Co-ions adsorbed on silica

Tatiana L. Rakitskaya [a,*], Alim A. Ennan [a], Irina V. Granatyuk [a], Alexander Yu. Bandurko [a], Gilbert G.A. Balavoine [b], Yurii V. Geletii [b,c], V.Ya.Paina [a]

[a] *Physical–Chemical Institute of Environment and Human Being Protection, Odessa State University, 2 Dvoryanskaya Street, Odessa-26, 270026 Ukraine*

[b] *Laboratoire de Chimie de Coordination, CNRS, 205 Route de Narbonne, F-31077 Toulouse Cedex, France*

[c] *Institute of Chemical Physics in Chernogolovka, RAN, Chernogolovka, 142432 Russia*

Abstract

Kinetics and mechanism of low-temperature ozone ($(5–50) \times 10^{-3}$ mol/m^3 in the gas–air mixture) decomposition by Co-catalysts supported on silica have been studied. Co-ions adsorbed on silica react with surface oxygen species, thus resulting in an active catalyst. Low concentrations of Co-ions form a monolayer on the surface. Their specific catalytic activity remained constant, but sharply decreased at higher concentrations due to a formation of polynuclear Co-complexes. Ozone decomposition may occur either as a stoichiometric or catalytic process, depending on the ozone and catalyst concentrations. The turnover number increases with ozone concentration reaching a saturation point. It also increases with Co-concentration in the beginning, but drops at a concentration $>1 \times 10^{-4}$ mol/g. The mechanism of the reaction is discussed.

Keywords: Catalysis: low-temperature; Cobalt; Ozone decomposition kinetics; Silica

1. Introduction

Ozone is one of the major pollutants of urban atmospheres and is often present in industrial exhaust gases. The cost of air pollution alone to human health has been estimated to be US$ 9.8 million a year in the Los Angeles area [1]. Ozone concentration in poorly vented rooms, for example, in the welding industry, is heightened and may reach up to 14 mg/m^3 [2,3]. This is significantly higher than recommended by the World Health Organization (0.1–0.2 mg/m^3). Ozone is a very strong oxidizing agent (under acidic conditions $E(O_3/O_2) = 2.07$ V [4]) and is able to react with practically any reducing organic or inorganic agent. The lungs are the most sensitive sites to toxic ozone exposure [5]. Local purification systems or individual gas-masks (respirators) can significantly minimize the ozone level in the air. Different substances, such as carbon fibrous materials, celites, various homogeneous and heterogeneous catalysts, have been reported to destroy ozone by different mechanisms, by either reacting stoichiometrically or catalytically [6–10]. However, in spite of numerous efforts and significant progress in ozone decomposition, the reported methods cannot be applied due to different reasons. The potentially applicable carbon fibrous materials destroy ozone catalytically [11–14]. Another approach is the use of transition metal complexes as catalysts

* Corresponding author. Tel.: +380+0482-44-32-93; fax: +380-0482-23-11-16

E-mail address: tanya@farlep.net (T.L. Rakitskaya)

0920-5861/99/$ – see front matter
PII: S0920-5861(99)00158-3

[15–20]. However, the low-temperature catalysis of ozone decomposition with supported metal complexes has been poorly studied. For example, $PdCl_2/CuCl_2$ on Al_2O_3 [19] and Mn^{2+} on activated carbon [20] have been reported to decrease the ozone level by up to 0.1 mg/m^3 at room temperature, while laminated graphite compounds with transition metal chlorides were active at elevated temperatures, $T > 60^\circ$C [21]. The catalysts based on Co(II) ions are known to be the most efficient in ozone decomposition [15,16], due to a facile regeneration of Co(III) by either water vapor or intermediate radicals having reducing properties. The catalytic activity of supported metal complexes is essentially influenced by the specific interactions with certain surface groups, and consequently by the nature of a support material [22]. In this work, we used silica as a support for Co-ions and studied the effect of different factors on the rate of ozone decomposition by this catalyst in order to optimize the conditions for its possible application (e.g. in a respirator).

2. Experimental

Catalysts were prepared by adsorption of Co(II)-ions on a silica surface from an aqueous solution of $Co(NO_3)_2 \cdot 6H_2O$ ('Reakhim', former USSR). Commercially precipitated silica (KSMG-type, from 'Reakhim', former USSR) with a specific surface area $S = 360$ m^2/g, $V_{micropores} = 0.35$ cm^3/g, and $V_{mesopores} = 0.20$ cm^3/g was beforehand fractionated to average particle-sizes of 0.5, 1.0, 2.0, and 3.0 mm. The specific surface area and pore volumes of the silica were determined by measuring the benzene concentration during its continuous desorption under dynamic conditions at 25°C from the surface of silica which was previously saturated by benzene in accordance with [23]. The collected data were treated with standard software. The pore distribution was found using the Tompson–Kelvin equation, and the specific surface area from the BET equation. In a typical procedure, 10 g of silica was kept under vigorous agitation for 2 h in 20 ml of aqueous solution with varied concentrations of Co(II) at 25°C until the establishment of the adsorption equilibrium. The pH of the aqueous solution was measured in the beginning and in the end of the adsorption with a standard glass electrode. Co–silica was washed once with distilled water and dried at 110°C until constant weight. The content of Co(II) in a prepared catalyst was determined with a standard atomic absorption technique with the 'Saturn' spectrometer (former USSR).

A gas–air mixture (GAM) with a desired ozone concentration was prepared with an ozone generator by the silent electric discharge of pre-purified air from dust and nitrogen oxides. Beforehand, the reactor ozone containing GAM was passed through an appropriate column with $CaCl_2$ to maintain constant humidity at $\varphi = 50\%$. In order to study the influence of the amount of adsorbed water (m_{H_2O}) on the series of samples, the samples were dried at 110°C until constant weight and then were kept in desiccators above sulfuric acid or water until desirable water contents were achieved: $m_{H_2O} = 0.015$, 0.030, 0.050 and 0.100 g/g. GAM humidity, φ(%), was maintained in the series of samples at 10, 28, 40 and 75%. The humidity was controlled by a psychrometer (a wet-and-dry-bulb thermometer). The ozone concentrations before, and after, the reactor (C^i and C^f) were measured mainly with a 'Cyclone' optical gas analyzer (former USSR, for $1.0–1 \times 10^4$ mg/m^3) with a minimum detectable ozone concentration of 1 mg/m^3 and relative error within 15%. A chemiluminescence gas analyzer (0.002–0.5 mg/m^3) was applied to study an initial period of the process where ozone concentration was low and the reaction rate changed rapidly Under steady-state conditions, the rate of ozone decomposition was calculated as $W = \omega(C^i – C^f)/m$, where ω is the volumetric flow rate and m the weight of the catalyst.

The reaction was studied in a vertical reactor thermostated at 20°C, with an inner diameter of 2.6 cm. GAM entered the reactor from the top with a volumetric flow rate of $\omega = 1.7 \times 10^{-5}$ m^3/s and with a typical linear velocity $U = 3.2$ cm/s. The residence time, τ', of GAM was adjusted by varying the height (and subsequently the weight) of the catalysts while maintaining a constant inner diameter of the reactor and the volumetric flow rate. The linear velocity of GAM was modified by using the reactors with different inner diameters.

A redox potential of Co(II)/Co(III) supported on SiO_2 and the oxidation state of Co-ions were estimated potentiometrically before, and immediately after, the reaction. A Pt-wire and a standard SCE electrode were immersed (a minimum of 25% of the length of

Pt-electrode) into the catalyst and the potential being measured by a routine potentiometer [24].

3. Results and discussion

In order to determine the range of conditions wherein the reaction of ozone decomposition takes place and to test the performance of the reactor, we studied the effect of different macrokinetic factors on the process rate. The initial reaction rate was found to be unchanged with:

1. the average grain diameter (d_g) of the catalyst in the range of 0.75–3.0 mm;
2. the increase of the residence time (τ') from 0.22 to 0.94 s (the catalyst weight changed from 2.5 to 15 g); and
3. the increase of the linear velocity (U) from 3.2 to 6.7 cm/s.

Under our typical experimental conditions with the average grain diameter $d_g = 0.75$ mm and the height of the catalyst layer $H = 2$ cm, the axial diffusion can be neglected as the condition $d_g/H \ll 1$ is fulfilled. The wall effects are also insignificant, if $D_{react}/d_g \geq 30$, which holds true under our experimental conditions ($D_{react}/d_g \sim 35$). Hence, in our reactors under typical experimental conditions and in accordance with [25], we have the plug-flow regime; both, retardation due to the internal diffusion (for d_g = 1–3 mm) and the external diffusion (for $U = 3.2$–6.7 cm/s) can be neglected. Thus, the observed rate of ozone decomposition is determined only by the rate of chemical interaction and the reaction proceeds in the kinetic regime.

The rate of ozone decomposition, W, and the activity of the catalyst was not constant in the course of the reaction. With an increase of the reaction time, the rate drops sharply and then slowly decreases to zero. These time dependences for various initial ozone concentrations (C^i) and the catalyst load $C_{Co(II)} = 5.5 \times 10^{-5}$ mol/g are shown in Fig. 1.

At higher catalyst concentrations, $C_{Co(II)} \geq 1.0 \times 10^{-4}$ mol/g, the rate was stabilized and the steady-state ozone decomposition appeared (Fig. 2, curves 3 and 4).

The data on the initial reaction rates and turnover numbers (see below) along with the characteristics of the used catalysts are collected in Tables 1 and 2. The initial reaction rate was found to increase linearly with

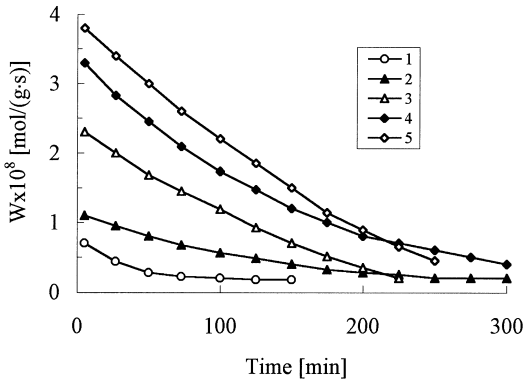

Fig. 1. Rates (W) of ozone decomposition catalyzed by supported Co(II)-ions against reaction time with different initial ozone concentrations, $C^i \times 10^2$, mol/m^3): 1–0.5; 2–1.0; 3–1.6; 4–3.1; 5–4.2. [Co(II)] = 5.5×10^{-5} mol/g; $T = 20$°C; humidity $\varphi = 50\%$; volume flow rate $\omega = 1.7 \times 10^{-5}$ m^3/s; linear velocity $U = 3.2$ cm/s.

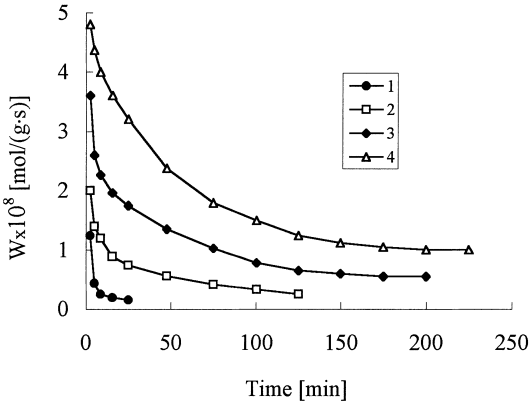

Fig. 2. Rates (W) of catalytic ozone decomposition against reaction time with different catalyst concentrations, [Co(II)] $\times 10^5$ mol/g: 1–2.0; 2–3.8; 3–10; 4–27. $C^i = 3.1 \times 10^{-2}$ mol/m^3; $T = 20$°C; humidity $\varphi = 50\%$; volume flow rate $\omega = 1.7 \times 10^{-5}$ m^3/s; linear velocity $U = 3.2$ cm/s.

the initial ozone (up to 2.6×10^{-2} mol/m^3) and catalyst (5.5×10^{-5} mol/g) concentrations. At their higher concentrations the rate growth decreases.

The transformation of the catalyst color from light-pink to dark-brown, and the shift of its redox potential from 0.28 to 0.915 V (against NHE) in the course of the reaction, signifies the oxidation of the initial Co(II) species by ozone to cobalt hydroxide $Co(OH)_3$ in accordance with the following reaction:

$$2Co(II) + O_3 + 2H^+ \rightarrow 2Co(III) + H_2O + O_2 \quad (I)$$

Table 1
Catalyst characteristics of the ozone decomposition and effect of the catalyst concentration[a]

$C_{Co(II)}$, $\times 10^5$ (mol/g)	α, $\times 10^{3}$[b]	β[c]	W_o[d] $\times 10^8$ (mol/g s)	A_s[e] $\times 10^8$ (mol/g s)	n[f]
2.0	0.7	0.16	1.2	7.5	1.0
3.8	1.33	0.32	2.2	6.9	3.0
5.5	1.93	0.46	3.5	7.6	8.0
10.0	3.5	0.83	3.7	4.5	3.0
19.6	6.88	1.60	4.6	2.9	3.0
27.0	9.48	2.20	4.9	2.2	1.0

[a] Reaction conditions: $T = 20^\circ$C; humidity $\varphi = 50\%$; volume flow rate $\omega = 1.7 \times 10^{-5}$ m^3/s; linear velocity $U = 3.2$ cm/s; initial ozone concentration $C^i = 3.1 \times 10^{-2}$ mol/m^3.
[b] The degree of surface coverage by the catalyst, Eq. (2).
[c] The saturation of absorption centers by metal ions, Eq. (3).
[d] Initial rate.
[e] Specific catalytic activity.
[f] Turnover number.

Table 2
Effect of initial ozone concentration C^i[a]

C^i, $\times 10^2$ (mol/m^3)	W_o,[b] $\times 10^8$ (mol/g s)	A_s[c] $\times 10^8$ (mol/g s)	n[d]
0.5	0.7	1.5	1.0
1.0	1.2	2.6	3.0
1.6	2.3	5.0	4.0
2.6	3.4	7.4	8.0
3.1	3.5	7.6	8.0
4.2	3.6	7.7	8.0

[a] Reaction conditions: $T = 20^\circ$C; humidity $\varphi = 50\%$; volume flow rate $\omega = 1.7 \times 10^{-5}$ m^3/s; linear velocity $U = 3.2$ cm/s; $C_{Co(II)} = 5.5 \times 10^{-5}$ mol/g
[b] Initial rate.
[c] Specific catalytic activity.
[d] Turnover number of the catalytic ozone decomposition.

This transformation of Co(II) to Co(III) was completely reversible. For example, if the catalyst of a dark-brown color was kept under air at 100°C for a duration of 12 h, its color was restored to its initial light-pink. Its redox potential also recovered to the initial value of 0.27 V. This catalyst always showed the same activity, even after several such regenerations (Fig. 3).

Furthermore, except for Co(II)-concentrations $\leq 2.0 \times 10^{-5}$ mol/g, the total amount of the decomposed ozone, Q_{ob}, always exceeds the theoretical value, Q_t, necessary to oxidize all of the Co(II) to Co(III). This unambiguously indicates the reduction of Co(III) back to Co(II) occurring simultaneously with reaction (1).

This is in agreement with results reported in Refs. [15,16], where ozone decomposition in the presence of cobalt salts was studied. This reaction was found to be catalytic in respect of Co-ions; the following mechanism being suggested:

$$Co^{2+} + O_3 + H_2O \rightarrow Co(OH)^{2+} + O_2 + OH^\bullet,$$

$$OH^\bullet + O_3 \rightarrow HO_2^\bullet + O_2,$$

$$HO_2^\bullet + Co(OH)^{2+} \rightarrow Co^{2+} + H_2O + O_2.$$

Thus, the foregoing proves the catalytic nature of ozone decomposition in our system, with the turnover number calculated as $n = Q_{ob}/Q_t$. The turnover number was >1 and increased with initial ozone and catalyst concentrations (see Tables 1 and 2). The steady-state regime of ozone decomposition establishes when the rate of Co(II) oxidation to Co(III) becomes equal to the rate of Co(II) reduction. Under these conditions, the rate of ozone decomposition does not depend on time. Such a steady-state decomposition took place at $C_{Co(II)} \geq 1.0 \times 10^{-4}$ mol/g and

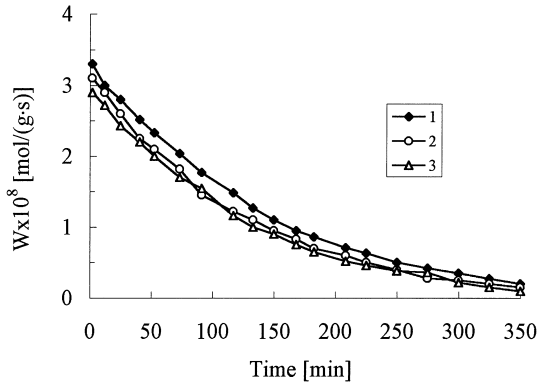

Fig. 3. Rates (W) of catalytic ozone decomposition against reaction time over freshly prepared (1) and regenerated catalyst (2 and 3, after the first and second regeneration, respectively). $C^{i} = 3.1 \times 10^{-2}$ mol/m^3; [Co(II)] = 5.5×10^{-5} mol/g; $T = 20^{\circ}$C; humidity $\varphi = 50\%$; volume flow rate $\omega = 1.7 \times 10^{-5}$ m^3/s; linear velocity $U = 3.2$ cm/s.

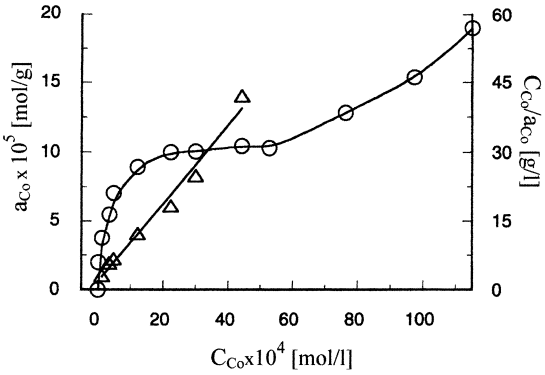

Fig. 4. The isotherm of Co(II) adsorption on silica (○) and its initial part in Langmuir coordinates (△), C_{Co}/a_{Co}–C_{Co}. C_{Co} is the equilibrium concentration of Co(II) in solution (mol/l); a_{Co} the amount of Co(II) adsorbed per unit of the adsorbent mass (mol/l), and $T = 20^{\circ}$C.

$C^{i} = 3.2 \times 10^{-2}$ mol/m^3 (see Fig. 2, curves 3 and 4). Since, at $C_{Co(II)} \geq 1.0 \times 10^{-4}$ mol/g, the steady-state regime is easily achieved and then the turnover number continuously increases, for simplicity, the value of n was taken at the time corresponding to the attainment of such a steady-state regime.

In order to explain the effect of catalyst concentration on the reaction rate, we looked at the isotherm of adsorption of Co(II) by silica (Fig. 4).

According to Giles' classification [26], the observed isotherm can be assigned to L_3 (Langmuir) class. It shows the multilayer formation of Co(II) on the silica surface at high catalyst concentrations. The initial portion of this isotherm fits the linear form of Langmuir isotherm, just like the adsorption of Cu(II)-ions by different silicas [27]:

$$\frac{C_{Co}}{a_{Co}} = \frac{1}{ba_m} + \frac{C_{Co}}{a_m}, \tag{1}$$

where C_{Co} is the equilibrium concentration of Co(II) in solution (mol/l), a_{Co} the amount of Co(II) adsorbed per unit of adsorbent mass (mol/g), a_m the limiting value of a_{Co}, (the monolayer capacity of the given adsorbent), in mol/g, and b a constant. The slope of the linear plot of C_{Co}/a_{Co} vs. C_{Co} (Fig. 4) gives $a_m = 1.2 \times 10^{-4}$ mol/g. In accordance with Kobozev's theory of active clusters [28] for metal-based catalysts adsorbed on the surface of a support, one can use the parameter α to characterize the 'degree of surface coverage' by Co-ions:

$$\alpha = \frac{N\sigma}{S} \tag{2}$$

where N is the total number of adsorbed Co(II) calculated from the value of a_m, σ the surface covered by one Co(II) ion (for the aqua complex of Co(II) $\sigma = 2.1 \times 10^{-20}$ cm^2), while S is the specific surface area of silica. The obtained low values of α (Table 1) lead to the conclusion that Co(II) adsorption occurs only on certain surface sites. The pH measurements before, and after, the adsorption procedure indicated the decrease of the pH value of the aqueous solution from 7.5 to 5.0 suggesting the ion-exchange reactions of Co(II) on the surface of silica:

$$\equiv\text{SiOH} + \text{Co}^{2+}_{(aq)} \rightleftarrows \left[\equiv\text{SiO–Co}^{2+}_{(aq)}\right]^{+} + \text{H}^{+} \qquad \text{(II)}$$

According to the method described in Ref. [29], we obtained the average ion-exchange constant to be $K_{Co^{2+}/H^{+}} = 4.4$, suggesting a strong binding of Co(II)-ion to the silica surface. The study of Co(II) desorption confirmed this conclusion. After the catalyst treatment by 1 M HCl at 20°C for 1 h, only 30% of the Co(II) was desorbed from the surface. From the data presented in Fig. 4, we found the parameter (β) which characterizes the saturation of absorption centers by metal ions under given conditions:

$$\beta = \frac{C_{Co(II)}}{a_m}, \tag{3}$$

where $C_{Co(II)}$ is the concentration of Co(II) on silica, and a_m the limiting value of $C_{Co(II)}$. It is clearly seen from Table 1 that, at $C_{Co(II)} > 1.2 \times 10^{-4}$ mol/g, multilayers of Co(II) are formed on silica accompanied with the decrease of specific catalytic activity, $A_s = W_0/\beta$. If only a monolayer of Co(II) is formed, then $\beta < 1$, and A_s remains constant. When $\beta > 1$, A_s drops sharply suggesting that the individual Co-ions are the catalytic centers in the ozone decomposition.

The preparation of the catalyst included its drying at relatively low temperatures (<110°C), and thus only weakly bound water can be removed under this condition [30]. Therefore, the Co(II) complex on silica surface may contain a coordinated water molecule and the catalytic active center can be presented as $[\equiv SiO–Co^{2+}(H_2O)_n]^+$. However, the same complex can be formed in the course of the reaction from the water present in GAM [22]. At high concentrations of Co(II), it forms polynuclear complexes (as associates or clusters) which are less active in ozone decomposition. The change in the number of water molecules in the inner coordination sphere of Co(II) could modify its catalytic activity. Indeed, the catalysts with different content of absorbed water showed different activity in ozone decomposition (Fig. 5).

In case of the sample dried at 110°C, a continuous decrease of reaction rate was observed (Fig. 5, curve 1). Whereas in the presence of water (Fig. 5, curves 2–5) the reaction rate sharply decreased, it reached a steady-state value and ozone decomposed with a constant rate for at least 3 h. However, at higher humidity of GAM ($m_{H_2O} = 0.1$ g/g), the steady-state regime was short and then the reaction rate decreased slowly. It is worth mentioning that the initial rate of ozone decomposition attributed to oxidation of Co(II) to Co(III) by ozone (reaction (I) became lower with increase of water content in GAM. At the same time, we believe that water promotes reduction of Co(III), thus, the steady state regime can be achieved easily. Co(III) reduction by water is thermodynamically feasible ($E_{Co(III)/Co(II)} = 1.81$ V, $E_{O_2/H_2O} = 1.23$ V).

Taking into account data available in the literature and that obtained in this study, the following mechanism of ozone decomposition ((III)-(VII))(Scheme 1) can be proposed:

According to this mechanism, the catalytic cycle includes:

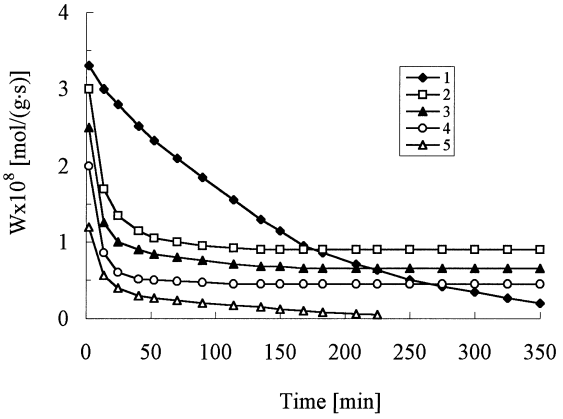

Fig. 5. Rates (W) of catalytic ozone decomposition against reaction time with different amounts of water adsorbed by the catalyst, m_{H_2O}, (g/g). (1), dried at 110°C; (2), 0.015; (3), 0.03; (4), 0.05, and (5), 0.10. $C^i = 3.1 \times 10^{-2}$ mol/m^3, [Co(II)] = 5.5×10^{-5} mol/g, $T = 20$°C; volume flow rate $\omega = 1.7 \times 10^{-5}$ m^3/s, and linear velocity $U = 3.2$ cm/s.

1. an oxidation of a starting Co(II) by ozone;
2. a regeneration of Co(III) by $HO_2^\bullet$ radical; and
3. a fast formation of $HO_2^\bullet$ from a hydroxyl radical and ozone.

Many other reactions can also occur, such as direct Co(III) reduction by water. Therefore, the proposed mechanism should be regarded as the simplest scheme to explain the catalytic effect of Co-ions, but not the comprehensive one.

Taking into account the electron configurations of Co(II) ($3d^7$) and O_3 [31], ozone can form a coordination bond with Co(II), donating a lone pair of electrons to Co(II) and by accepting electron density to its antibonding π^* orbitals (Reaction (III)). A similar mechanism has been observed by EPR in the reaction: $Ce^{3+} + O_3 \rightarrow \left[Ce^{4+} - O_3^-\right]$ [32]. A further transformation of the activated ozone and the water molecule in the coordination sphere is depicted in reaction (IV). This reaction probably occurs through the inner sphere transfer of an electron from Co(II) to ozone with a simultaneous proton transfer from coordinated water to ozone in the six-member transition state. For the first time, such an inner sphere mechanism, based on the analysis of thermodynamics and kinetics of Ag(I), Co(II), Mn(II), Ce(III), Ru(IV), Np(IV) oxidation by ozone, was proposed in Ref. [33]. Alternatively, this reaction might occur as the hydrogen

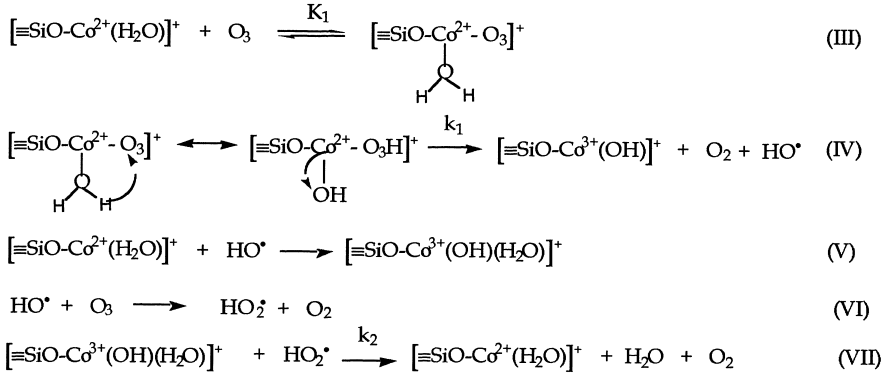

Scheme 1.

atom transfer from coordinated water to ozone. In this case, the electron is transferred from Co(II) to ozone through the bridging water molecule. Taking into consideration the data on ozone decomposition in water (pH ∼7), and in weak-alkaline solutions ($7 < pH < 12$) [34,35] as well as on Fe(II) oxidation by ozone [36,37], a fast decay of formed $HO_3^•$ gives free dioxygen and hydroxyl radical in reaction (IV). The hydroxyl radical is a very strong oxidizing agent and reacts either with Co(II) to give Co(III), or with ozone to produce $HO_2^•$ radical (reactions (V) and (VI), respectively). $HO_2^•$ and superoxide anion are both reducing species and are able to reduce Co(III) rapidly (reaction (VII), pK_a of $O_2^•$ in water is 4.8 [38], pH of the aqueous layer on the silica surface is estimated to be around 5).

We cannot exclude other pathways of Co(III) regeneration besides by $HO_2^•/O_2^•$ radicals. For example, at high ozone concentration or after a long exposure of the catalyst to ozone, the Co(II) species can be completely converted to Co(III). If so, reaction (V) becomes negligible and the recombination of hydroxyl radicals might take place to give hydrogen peroxide:

$$2HO^• \rightarrow H_2O_2 \quad \text{(VIII)}$$

Hydrogen peroxide can either reduce Co(III) itself or form such reducing species as $HO_2^•/O_2^•$ in the reaction with ozone and/or with hydroxyl radicals, thus ultimately regenerating Co(II). Reaction (VI) is unlikely to occur in the gas phase, since the hydroxyl radical must remain in the thin layer of adsorbed water on the silica surface. The yield of ozone decomposition reaction in the gas phase has been shown to occur only at elevated temperatures ($T > 60^\circ C$ [21]). Reaction (VI) competes with oxidation of Co(II) to Co(III) (reaction (V)) and becomes dominant at higher ozone concentrations, while being insignificant at low ozone concentrations. This kind of competition was studied in detail for the ozone decomposition catalyzed by iron(II) ions [36,37]. Under our experimental conditions, the competition of reactions (V) and (VI) affects the turnover number, *n*. In general, at high ozone concentrations, the decomposition is a catalytic process. The turnover number, *n*, can be as high as 8 before the establishment of a steady-state regime, whilst *n* is 1 at low ozone concentrations and the reaction becomes a stoichiometric one (Table 2). However, in spite of the increase of *n* at higher initial ozone concentrations, the rate of Co(II) regeneration in reaction (VII) might be too slow to achieve the steady state ozone decomposition, for example, at $[Co(II)]_o = 5.5 \times 10^{-5}$ mol/g. At high catalyst ($\geq 1 \times 10^{-4}$ mol/g) and ozone ($\geq 3.1 \times 10^{-2}$ mol/m^3) concentrations, the rate of Co(II) oxidation by ozone and its regeneration become equal, consequently the steady state regime establishes after 3 h of the reaction (Fig. 2, curves 3 and 4). The strong effect of water content on the rate of ozone decomposition (Fig. 5) suggests the important contribution of Co(III) reduction by water to the catalyst regeneration. Thus, ozone decomposition catalyzed by Co-ions adsorbed on silica is a very complicated process; nevertheless, the simplest mechanism depicted on Scheme 1 explains well all available experimental data.

4. Conclusions

The homogeneous ozone decomposition catalyzed by transition metal complexes in an aqueous solution is a rather well-studied reaction, but evidently it cannot be used for air purification. Whereas the supported transition-metal complexes are more feasible, they are not active enough and not well studied. We have found that Co(II) can be easily supported on the silica surface by the simple absorption method. Co(II) ions are strongly bound to silica by the ion-exchange mechanism with the estimated average ion-exchange constant $K_{Co^{2+}/H^+} = 4.4$. In the range of applied Co(II) concentrations, the surface was filled by catalyst only to a low value of $\alpha = (0.7–10) \times 10^{-3}$, suggesting the formation of isolated complexes on the silica surface. At room temperature, the prepared catalyst showed a high activity in ozone decomposition. The comparison of the isotherm of Co(II) adsorption on silica with the specific catalytic activity suggests that mononuclear Co(II) is the reactive site of ozone decomposition. Polynuclear complexes (clusters) are formed at $[Co(II)] > 1 \times 10^{-4}$ mol/g, but they have a low specific activity. The reaction pattern strongly depends on the initial ozone and cobalt concentrations. At low initial ozone and cobalt concentrations, the reaction is a stoichiometric process, while catalytic decay takes place at their higher concentrations. The proposed catalyst is believed to be potentially useful for its application for air purification.

5. List of symbols

a_{Co}	amount of Co (II) adsorbed per 1 g of unit of adsorbent (mol/g)
a_m	limiting value of a_{Co} (mol/g)
$A_s = W_0/\beta$	specific catalytic activity
b	constant of Langmuir equation
C_{Co}	equilibrium concentration of Co(II) in solution (mol/l)
C^f	final ozone concentration in GAM (mol/l)
C^i	initial ozone concentration in GAM (mol/l)
d_g	grain diameter (mm)
D_{react}	inner diameter of the reactor (mm)
	ozone redox potential in acid medium (V)
GAM	gas–air mixture
H	height of the catalyst layer (cm)
K_{Co^{2+}/H^+}	average ion exchange constant
KSMG	silica type
m	catalyst weight (g)
m_{H_2O}	amount of adsorbed water (g/g)
N	total number of adsorbed Co (II)
$n = Q_{ob}/Q_t$	turnover number
Q_{ob}	amount of decomposed ozone
Q_t	theoretical value of amount of decomposed ozone
S	specific surface area (m^2/g)
T	temperature (°C)
U	GAM linear velocity (cm/s)
W	rate of ozone decomposition (mol/g s)
W_0	initial rate, mol/(g s)
$V_{mesopores}$	specific volume of mesopores (cm^3/g)
$V_{micropores}$	specific volume of micropores (cm^3/g)
α	degree of surface coverage by Co-ions (a catalyst)
β	saturation of absorption centers by metal ions
φ	humidity (%)
τ'	effective residence time of GAM (s)
σ	surface covered by one Co(II) ion (cm^2)
ω	GAM volumetric flow rate (m^3/s)

Acknowledgements

We gratefully acknowledge the financial support from the Ministry of Education of Ukraine, and CNRS (France).

References

[1] J.W. Hall, A.M. Winer, M.T. Kleinmann, F.W. Lurman, V. Brajer, S.D. Colone, Science 255 (1992) 812.
[2] J. Medack, M. Roder, Schweisstechnik 37 (1987) 299.
[3] R. Knoch, Practicker, 42 (1990) 688.
[4] F.A. Cotton, G. Wilkinson, Advanced Inorganic Chemistry, Mir, Moscow, 1969, Part 2, 494 p.

[5] J.S. Tepper, D.L. Costa, J.R. Lehman, M.F. Weber, G.E. Hatch, Am. J. Respir. Dis. 140 (1989) 493.
[6] A.N. Nikonorov, Sources of Ozone in Exhausted Gases and Methods of its Removal, Khimneftemash, Moscow, 1985, p. 25.
[7] S. Imamura, M. Ikebata, T. Ito, T. Ogita, Ind. Eng. Chem. Res. 30 (1991) 217.
[8] A. Quederni, Q. Limvorapituk, R. Bes, I.C. Mora, Ozone Sci. Eng. 18 (1996) 385.
[9] B. Dhandapani, S.T. Oyama, Appl. Cat. B: Environm. 11 (1997) 129.
[10] Ch. Heisig, W. Zhang, S.T. Oyama, Appl. Cat. B. Environm. 14 (1997) 117.
[11] L.F. Atyaksheva, G.I. Emelyanova, Zh. Fiz. Khim. 63 (1989) 2606.
[12] T.L. Rakitskaya, E.K. Vasil'eva, A.Yu. Bandurko, V.Ya. Paina, Kinet. Catal. 35 (1994) 103.
[13] T.L. Rakitskaya, A.Yu. Bandurko, A.A.A. Ennan, V.V. Litvinskaya, Kinet. Catal. 35 (1994) 763.
[14] T.L. Rakitskaya, A.Yu. Bandurko, A.O.V. Boginskaya, Zh. Priklad. Khim. 69 (1996) 167.
[15] G.R. Hill, J. Am. Chem. Soc. 70 (1948) 1306.
[16] G.R. Hill, J. Am.. Chem. Soc. 71 (1949) 2434.
[17] G.P. Nikitina, A.Yu. Ivanov, V.G. Shumkov, V.P. Egorova, Radiokhim. 17 (1975) 957.
[18] N.D. Yordanov, Yu. Karadzhov, Transition Met. Chem. 10 (1985) 15.
[19] V.F. Zackay, D.R. Rowe, US Patent, 8,415,221, 1983.
[20] Japan Patent, N 53-45712, 1978.
[21] S.V. Osintseva, L.E. Gorlenko, G.I. Emelyanova, L.D. Kvatcheva, Yu.N. Novikov, M.E. Vol'pin, Zh. Fiz. Khim. 63 (1989) 3228.
[22] T.L. Rakitskaya, I.V. Granatyuk, G.G.A. Balavoine, Yu.V. Geletii, A.A. Golub, L.A. Rascola, Intern. Conf. 'Silica-98'. Mulhouse, France, 1–4 September, 1998, 653 p.
[23] G.I. Fedorov, R.I. Izmailov, in: The Porous Structure of Catalysts and Transport Processes in Heterogeneous Catalysis, IV International Congress on Catalysis, Symp. III, Nauka, Novosibirsk, 1970, p. 183.
[24] T.L. Rakitskaya, N.N. Abramova, Izv. Vyssh. Ucheb. Zaved. Khim. Khim. Tekhnol. 26 (1983) 1334.
[25] G.K. Boreskov, Catalysis, Nauka, Novosibirsk, 1971, parts 1 and 2, 268 p.
[26] G.D. Parfitt, C.H. Rochester (Eds.), Adsorption from Solution at the Solid/Liquid Interface, Academic Press, London, 1983, 460 p.
[27] G.C. Bye, M. McEvoy, M.A. Malati, J. Chem. Tech. Biotechnol. 32 (1982) 781.
[28] N.I. Kobozev, Selected Works, Moscow State University Publ., Moscow, 1978, 422 p.
[29] B.I. Nikolskii, V.I. Paramonova, A.N. Mosevich, Zh. Fiz. Khim. 34 (1960) 2664.
[30] C.J. Chisholm-Brause, P.A. O'Day, G.E. Brown Jr., G.A. Parks, Nature 348 (1990) 528.
[31] Y. Tanaka, E.C.Y. Inn, K. Watanabe, J. Chem. Phys. 21 (1953) 1651.
[32] A. Naydenov, R. Stoyanova, D. Mehandjiev, J. Mol. Catal. A: Chem. 98 (1995) 9.
[33] G.P. Nikitina, Radiokhimiya 17 (1975) 957.
[34] A. Virdis, A. Viola, G. Cao, Ann. Chim. Soc. Chim. Ital. 85 (1995) 633.
[35] P. Westerhoff, R. Song, G. Amy, R. Minear, Ozone-Sci. Eng. 19 (1997) 55.
[36] T.C. Yang, W.C. Neely, Anal. Chem. 58 (1986) 1551.
[37] T. Logarer, J. Holeman, K. Sehested, T. Pedersen, Inorg. Chem. 31 (1992) 3523.
[38] M. Tomijasu, H. Fukutomi, G. Gordon, Inorg. Chem. 24 (1985) 2962.